On the Homolytic Cleavage of the N,O Bond in *N*-(Methoxy)pyridine-2(1*H*)-thione and *N*-(Methoxy)thiazole-2(3*H*)-thione in Thermally and Photochemically Induced Reactions: A Theoretical Study

Mario Arnone,[†] Jens Hartung,[‡] and Bernd Engels*[,†]

Institute of Organic Chemistry, University of Würzburg, Am Hubland, D-97074 Würzburg, Germany, and Department of Chemistry, Organic Chemistry, University of Kaiserslautern, Erwin-Schrödinger-Straβe, D-67663 Kaiserslautern, Germany.

Received: December 22, 2004; In Final Form: May 12, 2005

The accuracy of theoretical approaches to describe electronic absorption spectra of *N*-(hydroxy)- and *N*-(methoxy)- derivatives of pyridine-2(1*H*)-thione and thiazole-2(3*H*)-thione are examined with the aim to identify methods that are applicable for a rational design of new photochemically active oxyl radical precursors. In addition, the mechanism of the photochemically induced methoxyl radical formation from *N*-(methoxy)-pyridine-2(1*H*)-thiones and of *N*-(methoxy)thiazole-2(3*H*)-thiones is investigated by means of theoretical methods. The results of the study are applied in order to explain differences in photoreactions of *N*-(alkoxy)-pyridine-2(1*H*)-thiones and the corresponding thiazole-2(3*H*)-thiones.

Introduction

Oxygen-centered radicals are important intermediates in photobiological,[1−3] mechanistic,[4,5] and synthetic studies.[6] The majority of methods for a generation of reactive oxyl radicals relies on homolytic cleavages of O,O bonds in organic peroxides or peresters.[7−9] Most precursors of this type are, however, labile and thus delicate to handle. Therefore, *O*-alkyl derivatives of *N*-(hydroxy)pyridine-2(1*H*)-thione (**1a**) (Figure 1) and, in particular, of 4- and 4,5-substituted *N*-(hydroxy)thiazole-2(3*H*)-thiones (i.e., derivatives of **2**) have attracted considerable attention for this purpose in the past few years.[10,11]

In a previous work we have reported on the synthesis of 4- and 4,5-substituted *N*-(methoxy)thiazole-2(3*H*)-thiones. Their electronic spectra were recorded in order to systematically probe effects of alkyl and aryl substituents on low energy absorption bands of these compounds.[12] In addition, a study on the UV/vis spectral properties of pyridine-2(1*H*)-thione **1a** and **1b** has been performed.[12] The experimentally observed UV/vis bands of compounds **1a**−**b** were reproduced using time-dependent density functional theory (TD-DFT)[13,14] in association with the BLYP[15,16] or the B3LYP[17] functional. The experimental spectrum of *N*-(methoxy)pyridine-2(1*H*)-thione **1b** in EtOH shows two broad bands with maxima located at 3.45 and 4.31 eV. On the basis of computed transition energies and oscillator strengths, we assigned the lower energy band to the $S_0 \rightarrow S_2$ excitation ($\pi_{CS} \rightarrow \pi_{ring}$).[12] The experimental spectrum of *N*-(methoxy)-4-methylthiazole-2(3*H*)-thione, i.e., the 4-methyl derivative of thiazolethione **2b**, shows one band with a maximum at 3.87 eV (in EtOH), which we correlated with the $S_0 \rightarrow S_2$ transition ($\pi_{CS} \rightarrow \pi_{SCS}$). The lowest energy band in the experimental spectra of 4- or 5-aryl *N*-(methoxy)thiazole-2(3*H*)-thiones shows a red shift with respect to *N*-(methoxy)-4-methylthiazole-2(3*H*)-thione but mainly possesses the same character. The computed UV/vis spectral properties of the latter compound are similar to those of *N*-(methoxy)thiazole-2(3*H*)-thione (**2b**), a compound that has, however, hitherto not been prepared. In view of the chemistry associated with an excitation of the energetically lowest band, it is very likely that a population of the S_2 state is associated with the succeeding N,O homolysis in *N*-(methoxy)-4-methylthiazole-2(3*H*)-thione and probably also in thiazolethione **2b** and pyridinethione **1b**.

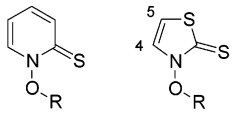

1 **2**

1, **2**	R
a	H
b	CH_3

Figure 1. Structural formulas and indexing of pyridine-2(1*H*)-thiones **1** and thiazole-2(3*H*)-thiones **2**.

While the BLYP and the B3LYP functionals provided matching results with respect to the assignment of the individual transitions, the predicted vertical excitation energies differed considerably. For *N*-(methoxy)thiazole-2(3*H*)-thiones (**2b**) the prediction of BLYP for the excitation energy to the S_2 state agrees nicely with the maximum of the lowest band of the experimental spectrum, while computations performed with the B3LYP functional deviate by more than 0.3 eV. For *N*-(methoxy)pyridine-2(1*H*)-thione (**1b**) BLYP underestimates the excitation energy by about 0.5 eV while the results from B3LYP computations agree nicely. Furthermore, since S_1 and S_3 represent dark states it is unclear whether these agreements only hold for the respective S_2 states.

Despite their similarities, *N*-(alkoxy)pyridine-2(1*H*)-thiones and *N*-(alkoxy)-4-methylthiazole-2(3*H*)-thiones behave surprisingly different if photolyzed in the absence of trapping reagents. Thus, *N*-(4-penten-1-oxy)pyridine-2(1*H*)-thiones undergo highly efficient rearrangements to provide 2-(2-tetrahydrofurylmethylsulfanyl)pyridines under such conditions. *N*-(4-Penten-1-oxy)-thiazole-2(3*H*)-thiones, on the other hand, react surprisingly

* Corresponding author. E-mail: bernd@chemie.uni-wuerzburg.de.
[†] University of Würzburg.
[‡] University of Kaiserslautern.

10.1021/jp044163b CCC: $30.25
Published on Web 06/15/2005

sluggish and give rise to several unwanted side products if photolyzed in an inert solvent.[11] To improve the characteristics of a future generation of *N*-(alkoxy)thiazole-2(3*H*)-thiones as a powerful and versatile oxyl radical precursor, it is important to understand the differences in photophysical events associated with near UV/vis excitation of cyclic thiohydroxamic acid O-esters in general. Therefore, we have explored the mechanism of N,O homolysis in *N*-(methoxy) compounds **1b** and **2b** using theoretical approaches.

Modern computational chemistry offers a considerable diversity of methods for describing electronically excited states. The Multi-Reference Configuration Interaction method (MR-CI)[18,19] and an approach which combines the Complete Active Space approach (CASSCF)[20,21] to account for the near-degeneracy effects with a perturbational treatment in second order to include dynamical correlation (CASPT2) approaches[22,23] are known for the prediction of very accurate vertical excitation energies and are well suited to describe photochemical reactions. They are too time-consuming, however, to be applied for the design of new 4- and 4,5-substituted *N*-(alkoxy)thiazole-2(3*H*)-thiones.

TD-DFT approaches are fast enough for this purpose; however, the achieved accuracies are considerably lower. For example TD-DFT in combination with the commonly applied exchange correlation (XC) functionals is known to possess problems to describe charge-transfer transitions or Rydberg states precisely.[24−26] Fabian and co-workers have demonstrated that the TD-DFT approach in association with a hybrid functional is able to describe electronic excitations involving the thiocarbonyl chromophore[27] being one of the chromophores of *N*-(alkoxy)thiazole-2(3*H*)-thiones and N-(alkoxy)pyridine-2(1*H*) thiones. The effects of substituents at the thiocarbonyl carbon atom on the energetic positions of the n $\rightarrow \pi^*$ and the $\pi \rightarrow \pi^*$ excitation were reproduced with an excellent precision. Even if a considerable intramolecular charge transfer from a donor group to the thiocarbonyl acceptor group occurs, the transition energies are not that erratic as in the case of other intramolecular charge-transfer transitions. Our previous study indicates,[12] however, that this may not always be the case for *N*-(alkoxy)thiazole-2(3*H*)-thiones and *N*-(alkoxy)pyridine-2(1*H*) thiones.

A very attractive approach is the CC2 model.[28] It represents an approximation of the Coupled Cluster method including single and double excitation (CCSD) and gives excitation energies for single excitations correct through second order in the electron fluctuation potential. If the wave function of the excited state is dominated by single replacements out of the reference determinant, CC2 gives vertical excitation energies typically correct within 0.3 eV[19,29,30] but often an accuracy of 0.1 eV is found.[31] Combining the CC2 model with the RI approximation[32,33] (RI-CC2) the CC2 model gets very efficient[34,35] and can be employed for rather large molecules. Besides its efficiency it has the advantage that it describes charge-transfer states correctly.

The first aim of the present study is to uncover theoretical approaches that are adequate to reproduce the experimental UV/vis spectral characteristics of pyridine-2(1*H*)-thiones **1a**−**b** and of thiazole-2(3*H*)-thiones **2a**−**b**. In the first part of the paper TD-DFT approaches, the RI-CC2 method, and the CASPT2 approach are tested for this purpose. The second aim is to investigate the mechanism of N,O homolysis in *N*-(methoxy) compounds **1b** and **2b** using the CASPT2 method. In addition, we have tested to what extent the other approaches used in this study are able to describe the photolytic dissociation process. Since photochemically induced reactions of *N*-(alkoxy)thiazole-2(3*H*)-thiones are initiated via UV/vis absorption at the lower energy end of their spectra, in this part of our investigations we have focused on states possessing vertical excitation energies up to 4.0−4.2 eV.

Theoretical Details

All DFT, TD-DFT, and RI-CC2 calculations were performed with the TURBOMOLE program package[36] while CASSCF[20,21] and CASPT2[22,23] computations were performed with the MOLCAS program.[37]

All vertical excitation energies were computed for theoretically determined ground-state geometries. They were obtained with the BLYP/SVP approach[15,16,38] applying the resolution of identity (RI) approximation.[32,33] This approximation is included since it is often the only practical tool if many and large molecules shall be screened. To study resulting errors vertical excitation energies were also computed for ground-state geometries obtained with the RI-MP2/cc-pVTZ approach.[39] CASSCF computations for calculating vertical excitation energies were done with different CAS spaces (see text). For the PT2 computations the G3 approach[40] for the fock matrix and the multi-state variant (MS-CASPT2)[41] were used. For these computations the cc-pVTZ basis sets[42,43] were applied on all atoms except for the hydrogen atoms and the methoxy carbon atom in *N*-(methoxy)pyridine-2(1*H*)-thione **1b**. These atoms had to be described with cc-pVDZ basis sets[42,43] due to software and hardware limitations. Computations in which the cc-pVTZ bases were enlarged by diffuse functions (2s,2p, see below) failed due to hardware limitations. We estimated their influence by computations employing the smaller TZVP basis with and without one diffuse (sp) set. This approximation seems to be valid since all approaches showed nearly the same influence of the diffuse functions.

Oscillator strengths within the CAS approach were obtained with the RAS state interaction program (RASSI)[44] together with the 12/12 CAS space. In these computations the cc-pVDZ basis sets were used due to limitations in the computer resources. For time dependent density functional theory (TD-DFT) methods[13,14] and the RI-CC2,[34,35] ansatz TZVP[45] and cc-pVTZ[42,43] basis sets (together with the matching auxiliary basis sets[32,39] in case of RI calculations) were applied. Additionally, we tested the influence of diffuse functions. To the TZVP basis we added an s and a p function. To the cc-pVTZ basis two s and two p functions were added (see Supporting Information). Within TD-DFT the BLYP, the B3LYP, the BHLYP,[46] and the PBE0[47,48] functionals were applied. For BLYP calculations, the RI approximation in the time dependent formalism (RI TD-DFT)[49] was used. For the computations with diffuse functions the auxiliary basis sets were modified according to ref 50.

For a description of the N,O cleavage, all internal degrees of freedom of the molecules were optimized at defined fixed N,O distances using the B3LYP/SVP level of theory since the energy positions of S_1 and S_2 seem to be little influenced by the chosen ground-state geometries. This was done for the S_0 ground state and the first triplet state (T_1). For the S_0 geometry, a biradical wave function ($<S^2> = 1$) had to be used at a N,O distance of 2.25 Å in order to describe the correct fragmentation channel. In our computations this was achieved with a triplet density matrix as an initial guess. In the following, computations, which involve an optimized geometry for a triplet state, will be abbreviated as $T_1//T_1$, $S_1//T_1$, etc (i.e., state//optimized geometry). Computations, which use the ground-state geometries, are given as $S_0//S_0$, $T_1//S_0$, etc. For CASSCF and CASPT2, an (16/

TABLE 1: CASPT2 Results of Vertical Excitation Energies; All Values in eV

N-(Methoxy)pyridine-2(1*H*)thione (**1b**)[a]					
	12/12 CAS space ((s.o.))			16/12 CAS space	
state	CAS	CASPT2	MS−CASPT2	CAS	CASPT2
S_1	2.72/3.30[b]	2.89/2.95	2.97/3.03	3.12	2.87
S_2	3.45/3.82	3.09/ 3.08	3.27/3.24	3.83	3.04
S_3	3.90/4.49	3.71/3.67	3.80/3.77		

N-(Methoxy)thiazole-2(3*H*)-thione (**2b**)[c]					
	12/12 CAS space			16/12 CAS space	
state	CAS	CASPT2	MS-CASPT2	CAS	CASPT2
S_1	3.77/3.62	3.54/3.51	3.63/3.63	3.73	3.55
S_2	4.80/4.85	3.68/3.66	3.86/3.90	4.86	3.83
S_3	5.00/5.05	4.42/4.51	4.52/4.63		

[a] The experimental spectrum (in ethanol) shows two broad bands with maxima at 3.45 and 4.31 eV. [b] The ground state geometries were determined with RI-BLYP/SVP (left values) and with RI-MP2/cc-pVTZ (right values), respectively. The right values also include the influence of diffuse functions (see text). [c] The experimental spectrum of *N*-(methoxy)-4-methylthiazole-2(3*H*)-thione (in EtOH), i.e., the 4-methyl derivative of thione **2b**, shows a broad band with a maximum at 3.87 eV.

12) active space is necessary in order to describe N,O homolyses out of the S_0, S_1, and S_2 states because during the bond breaking process a strong mixing between these orbitals occurs. With a smaller CAS space (e.g., in a 12/12 CASSCF) a reliable description of the S_1 and S_2 states is not possible. Since diffuse functions seem to have little influence on the energy position of S_1 and S_2, cc-pVTZ basis sets were used. The S_1 state was in addition optimized using the TD-DFT gradient[51] (B3LYP/SVP) that is implemented in TURBOMOLE. However, such optimizations were only possible up to a N,O distance of 1.6 Å. For larger bond distances the computations did not converge. In this region, the $S_1//S_1$ curve for both molecules is slightly lower in energy than the $S_1//T_1$ curve, but both are quite parallel (0.1−0.2 eV on the BLYP/TZVP or B3LYP/TZVP level of theory; see Supporting Information). This indicates that T_1 geometries represent reasonable approximations for S_1 states in this study, at least as long as both fragments interact with each other ($R_{N,O}$ = 1.368−2.25 Å; see below). For the description of the noninteracting methoxyl radical ($R_{N,O}$ > 4.0 Å), we used the results of Höper et al.[52] who applied large scale MR−CI calculations.

Results and Discussions

Comparison of the Ability of Different Theoretical Approaches to Compute Vertical Excitation Energies. The results of CASPT2 computations for vertical electronic excitations of *N*-(methoxy)pyridine-2(1*H*)-thione (**1b**) and *N*-(methoxy)thiazole-2(3*H*)-thione (**2b**) using a CAS space consisting of 12 electrons and 12 orbitals (12/12 CAS) are summarized in Table 1. The corresponding ground-state geometries were determined with the RI-BLYP/SVP method (left values) and with the RI-MP2/cc-pVTZ method (right value). The RI-MP2/cc-pVTZ ground state geometries are slightly more compact; e.g., all bond distances decrease by about 0.02 Å (see Supporting Information). Table 1 also contains the 16/12 CASPT2 data. The latter information is required to describe the photochemically induced dissociation processes (see below; for data using smaller CAS spaces, see Supporting Information). The results shown in Table 1 underline the importance of the use of PT2 to obtain reliable excitation energies; however, the differences between the normal (G3 ansatz) and the MS variant are generally

TABLE 2: Excitation Energies for the Methoxy Compounds Obtained with Various Approaches; All Values in eV

N-(Methoxy)pyridine-2(1*H*)-thione (**1b**)[a]						
	CASPT2[b]	BLYP	B3LYP	BHLYP	PBE0	RI-CC2
S_1	2.97/3.03	2.24/2.28[c]	2.77/2.83	3.32/3.41	2.91/2.98	3.13/3.18
S_2	3.27/3.24	2.96/2.98	3.33/3.35	3.79/3.83	3.45/3.48	3.60/3.62
S_3	3.80/3.77	3.04/3.05	3.58/3.55	4.61/4.55	3.76/3.73	4.02/3.93

N-(Methoxy)thiazole-2(3*H*)-thione (**2b**)[d]						
	CASPT2[b]	BLYP	B3LYP	BHLYP	PBE0	RI-CC2
S_1	3.63/3.63	3.27/3.24[c]	3.48/3.50	3.74/3.81	3.57/3.61	3.74/3.76
S_2	3.86/3.90	3.84/3.81	4.16/4.11	4.46/4.41	4.26/4.22	4.19/4.13
S_3	4.52/4.63	3.96/3.99	4.40/4.44	4.96/4.99	4.54/4.61	4.73/4.73

[a] The experimental spectrum (in EtOH) shows two broad bands with maxima at 3.45 and 4.31 eV. [b] The values correspond to the MS-CASPT2 results summarized in Table 1. [c] Left values: ground state geometries determined with RI-BLYP/SVP; excitation energies computed with the TZVP basis sets. Right values: ground state geometries determined with RI-MP2/cc-pVTZ; excitation energies computed with the cc-pVTZ basis sets augmented with diffuse functions (see text and Supporting Information). [d] The experimental spectrum of *N*-(methoxy)-4-methylthiazole-2(3*H*)-thione (in EtOH), i.e., the 4-methyl derivative of thione **2b**, shows a broad band with a maximum at 3.87 eV.

≤0.1 eV. For the S_2 state of thiones **1b** and **2b**, a difference of 0.2 eV is found, indicating some mixing. Slightly lower excitation energies (0.1 eV) were obtained upon the use of a 16/12 instead of a 12/12 space.

Compared to the upper approach for **1b** the CASPT2 or MS-CASPT2 values change less than 0.1 eV if the vertical excitation energies are computed for the RI-MP2/cc-pVTZ ground state geometries and if the influence of diffuse functions is included (see below for a more detailed discussion). For the CAS calculations considerably higher deviations are found, however. For S_1 and S_2 of **2b** the RI-MP2/cc-pVTZ ground state geometries lead to slightly higher excitation energies (<0.1 eV). The vertical excitation energy to the S_3 state increases by about 0.3 eV.

The predictions of Time Dependent Density Functional Theory (TD-DFT) approaches and of the RI-CC2 method for *N*-(oxy)-substituted pyridine-2(1*H*)-thiones **1** and the corresponding thiazole-2(3*H*)-thiones **2** are summarized in Table 2. As for Table 1 the left values summarizes the predictions obtained in combination with the RI-BLYP/SVP ground-state geometries. They were computed with the TZVP basis set. For the right values, the RI-MP2/cc-pVTZ ground state geometries were employed. Additionally, we used the cc-pVTZ basis sets augmented with diffuse basis functions (see Supporting Information for a listing of all computations). The corresponding MS-CASPT2-G3 values are given for comparison.

For all methods the deviations between both approaches are less than 0.1 eV. For all states of **1b** and the S_1 and S_2 state of **2b**, this results since all changes (change in basis set and geometries, inclusion of diffuse basis functions) do not effect the excitation energies considerably (<0.1 eV). For the S_3 state of **2b**, however, the small deviations result since geometry effects and basis set effects cancel each other to some extent. The change in the geometry leads to higher excitation energies of about 0.15−0.25 eV while a decrease of about 0.15−0.2 eV results from the inclusion of diffuse functions. The influence of the (sp)-basis (cc-pVTZ vs TZVP) is small (<0.1 eV) as expected. A complete listing of all computations can be taken from the Supporting Information.

MS-CASPT2-G3 and RI-CC2 agree within the expected uncertainties of both approaches.[19,29−31] For the S_2 states of **1b** and **2b**, RI-CC2 predicts higher excitations by about 0.3 eV

TABLE 3: Computed Oscillator Strength [10^{-2} Arb. Units]

	[a]*N*-(Methoxy)pyridine-2(1*H*)-thione (**1b**)					
	CASSCF[b]	BLYP	B3LYP	BHLYP	PBE0	RI-CC2
S_1	0.03	<0.01/<0.01[c]	<0.01/<0.01	0.02/0.02	0.01/<0.01	<0.01/<0.01
S_2	9.19	2.51/2.29	5.14/4.60	12.7/11.6	6.09/5.36	12.6/10.6
S_3	0.03	0.06/0.06	0.06/0.06	0.04/0.14	0.06/0.06	0.04/0.05
	N-(Methoxy)thiazole-2(3*H*)-thione (**2b**)[d]					
	CASSCF[b]	BLYP	B3LYP	BHLYP	PBE0	RI-CC2
S_1	<0.01	0.01/0.03	0.01/0.02	0.02/0.02	0.01/0.02	0.01/0.03
S_2	26.4	5.20/7.44	13.3/14.4	19.9/20.8	15.0/16.0	23.9/24.1
S_3	0.03	0.06/0.09	0.06/0.12	0.07/0.17	0.06/0.13	0.10/0.17

[a] The experimental spectrum (in ethanol) shows two broad bands with maxima at 3.45 and 4.31 eV. According to our CASPT2 computations the maxima at 3.45 eV is assigned to the S_2 state. [b] The 12/12 CASSCF space together with the cc-pVDZ basis sets was applied. [c] Left values: ground state geometries determined with RI-BLYP/SVP; oscillator strength computed with the TZVP basis sets. Right values: ground-state geometries determined with RI-MP2/cc-pVTZ; oscillator strength computed with the cc-pVTZ basis sets augmented with diffuse functions (see Supporting Information). [d] The experimental spectrum of *N*-(methoxy)-4-methylthiazole-2(3*H*)-thione (in EtOH), i.e., the 4-methyl derivative of thione **2b**, shows a broad band with a maximum at 3.87 eV, which, according to our CASPT2 computations, was assigned as the transition to the S_2 state.

while the deviation for the S_1 and S_3 states is 0.2 eV or less. The MS-CASPT2-G3 values computed for **2b** agree better to the maxima of the lowest bands measured for *N*-(methoxy)-4-methylthiazole-2(3*H*)-thione, i.e., the 4-methyl derivative of thione **2b** (3.87 eV). However it is important to note that the band is broad and that the influence of the vibrational structure is unknown. The methyl substituent is not expected to influence this band. For **1b** the predictions of both methods for the vertical excitation energy to S_2 bracket the experimental maximum of the lowest band (3.45 eV).

The agreement between these two methods and the various TD-DFT approaches depends strongly on the type of TD-DFT approach and the state under consideration. The BHLYP functional generally strongly overestimates the excitation energies (0.5−0.6 eV with respect to MS-CASPT2-G3), except for the S_1 state of **2b**, for which it agrees within a precision of 0.1 eV to the MS-CASPT2-G3 results. The BLYP functional on the other hand considerably underestimates all excitation energies (up to 0.8 eV). Only the predicted location of the S_2 state of *N*-(methoxy)thiazole-2(3*H*)-thione **2b** is in excellent agreement with the MS-CASPT2-G3 result and with the maximum of the observed broad band. This agreement may originate from a cancellation of errors, since all other TD-DFT approaches overestimate this excitation energy considerably. The PBE0 functional agrees nicely with MS-CASPT2. Except for the S_2 states of both molecules, the deviations with respect to the MS-CASPT2-G3 are less than 0.1 eV. For both S_2 states the deviations are 0.2 eV (for **1b**) and 0.4 eV (for **2b**). The fact that these states dominate the experimental UV/vis spectra limits the applicability of this functional for the study of substituent effects to some extent. Besides the PBE0, the B3LYP functional performs reasonably since for S_1 and S_2 states it deviates by only 0.1−0.2 eV from the MS-CASPT2-G3 results. For the S_2 state of *N*-(methoxy)pyridine-2(1*H*)-thione **1b** it possesses the best agreement with the maximum of the measured broad band.

The computed oscillator strengths for transitions in thiones **1** and **2** are summarized in Table 3. All approaches agree that only excitations to the S_2 show nonvanishing transition probabilities in the near-UV region. The absolute values differ by a factor of 5.

The calculated excitation energies for *N*-(hydroxy)pyridine-2(1*H*)-thione **1a** and *N*-(hydroxy)thiazole-2(3*H*)-thione **2a** are summarized in Table 4. With respect to the influence of basis set size and ground state geometries, **1a** and **2a** possess somewhat stronger dependencies than **1b** and **2b** (Table 2). The oscillator strengths associated with the transitions of **1a** and **2a** are listed in Table 5. The major structural difference between *N*-(methoxy)-substituted thiones **1b** and **2b** and *N*-(hydroxy) compounds **1a** and **2a** originates from an intramolecular hydrogen bond between the hydroxyl group and the thiocarbonyl sulfur atom. This computed structural feature is seen in the solid-state geometry of **1a**. The derivatives of **2a** that have so far been studied by X-ray diffraction show intermolecular hydrogen bonding.[12] Hydrogen bonding in thiones **1a** and **2a** leads to a stabilization of the n-orbitals at sulfur. All methods except the BLYP functional predict that this interaction leads to an interchange of the S_1 and S_2 states in *N*-(hydroxy)pyridine-2(1*H*)-thione **1a**, if compared to *N*-(methoxy) derivative **1b**. Going from *N*-(methoxy)thiazole-2(3*H*)-thione **2b** to *N*-(hydroxy)-thiazole-2(3*H*)-thione **2a**, only the RI-CC2 predicts an interchange of the S_1 and S_2. However, for **2a** all methods predict that the energy separation of both states is less than 0.1 eV.

TABLE 4: Excitation Energies for the *N*-(Hydroxy) Compounds 1a and 2a Obtained with Various Approaches; All Values in eV

	N-(Hydroxy)pyridine-2(1*H*)-thione (**1a**)[a]					
	CASPT2[b]	BLYP	B3LYP	BHLYP	PBE0	RI-CC2
S_1	3.17/3.28	3.04/3.05[c]	3.44/3.48	3.92/3.97	3.56/3.61	3.63/3.71
S_2	3.55/3.75	3.06/3.10	3.55/3.59	4.15/4.23	3.71/3.76	3.91/3.95
S_3	4.35/4.32	3.70/3.73	4.23/4.20	4.80/4.78	4.41/4.37	4.45/4.47
	N-(Hydroxy)thiazole-2(3*H*)-thione (**2a**)[d]					
	CASPT2[b]	BLYP	B3LYP	BHLYP	PBE0	RI-CC2
S_1	3.92/4.02	3.74/3.75[c]	3.99/4.05	4.31/4.42	4.10/4.17	4.21/4.21
S_2	4.08/4.20	3.88/3.85	4.19/4.17	4.49/4.48	4.29/4.27	4.31/4.36
S_3	4.58/4.89	3.99/4.00	4.47/4.48	5.08/5.07	4.61/4.66	4.83/4.80

[a] The experimental spectrum (in ethanol) shows two broad bands with maxima at 3.57 and 4.40 eV. [b] Left values: ground state geometries were determined with RI-BLYP/SVP; excitation energies were computed with cc-pVTZ basis sets. Right values: ground state geometries were determined with RI-MP2/cc-pVTZ; excitation energies were computed with the cc-pVTZ basis. The influence of diffuse functions was estimated with the help of TZVP computations (see text). [c] Left values: ground state geometries determined with RI-BLYP/SVP; excitation energies computed with the TZVP basis sets. Right values: ground state geometries determined with RI-MP2/cc-pVTZ; excitation energies computed with the cc-pVTZ basis sets augmented with diffuse functions (see Supporting Information). [d] The experimental spectrum of *N*-(hydroxy)-4-methylthiazole-2(3*H*)-thione (in EtOH), i.e., the 4-methyl derivative of thione **2a**, shows a broad band with a maximum at 3.94 eV.

Assuming that the excitations which dominate the low energy spectrum are mainly located in the heterocyclic subunits of both

TABLE 5: Computed Oscillator Strength [10^{-2} Arb. Units]

	N-(Hydroxy)pyridine-2(1*H*)-thione (**1a**)[a]					
	CASSCF[b]	BLYP	B3LYP	BHLYP	PBE0	RI-CC2
S_1	10.5	<0.01/<0.01[c]	3.95/3.51	10.1/9.12	4.66/4.07	8.86/7.28
S_2	0.02	1.91/1.76	<0.01/<0.01	<0.01//<0.01	<0.01/<0.01	<0.01/<0.01
S_3	<0.01	<0.01/<0.01	<0.01/0.01	24.5//27.5	<0.01/0.02	29.0/31.7
	N-(Hydroxy)thiazole-2(3*H*)-thione (**2a**)[d]					
	CASSCF[b]	BLYP	B3LYP	BHLYP	PBE0	RI-CC2
S_1	<0.01	0.02/0.02	0.02/0.03	0.02/0.03	0.02/0.02	27.2/26.2
S_2	31.3	11.1/10.8	17.7/17.5	23.4/23.5	19.2/18.8	0.02/0.03
S_3	<0.01	<0.01/0.06	0.01/0.11	0.02/0.26	0.01/0.11	0.02/0.26

[a] The experimental spectrum (in EtOH) shows two broad bands with maxima at 3.57 and 4.40 eV. According to our CASPT2 computations the maxima at 3.57 eV is assigned to the S_1 state. [b] The 12/12 CASSCF space together with the cc-pVDZ basis sets was applied. [c] Left values: ground-state geometries determined with RI-BLYP/SVP; oscillator strength computed with the TZVP basis sets. Right values: ground state geometries determined with RI-MP2/cc-pVTZ; oscillator strength computed with the cc-pVTZ basis sets augmented with diffuse functions (see Supporting Information). [d] The experimental spectrum of *N*-(hydroxy)-4-methylthiazole-2(3*H*)-thione (in EtOH), i.e., the 4-methyl derivative of thione **2a**, shows a broad band with a maximum at 3.94 eV, which, according to our CASPT2 computations, was assigned to the transition to the S_2 state.

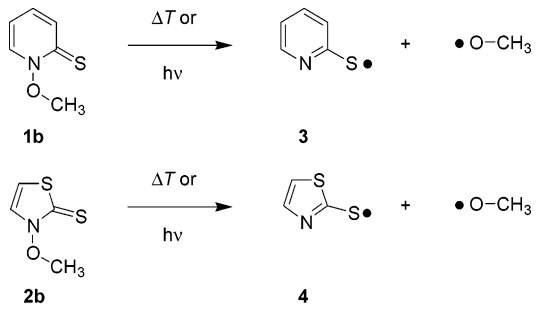

Figure 2. Product formation via N,O homolysis in *N*-(methoxy)-pyridine-2(1*H*)-thione **1b** and *N*-(methoxy)thiazole-2(3*H*)-thione **2b**.

compounds, a study about the influence of substituents on the absorption spectra of thiazolethione compounds could be performed with the BLYP functional: It predicts the near-UV transition into the S_2 state correctly, and it is so efficient that many large compounds can be investigated quite easily. However, for systems in which S_1 and S_3 gain oscillator strength due to substituent effects, the BLYP becomes too inaccurate. To obtain reliable descriptions for the S_1 and S_3 state, from TD-DFT approaches, the B3LYP functional or the PBE0 functional may be applied. However, both are less accurate for the S_2 state. The RI-CC2 approach represents a very attractive choice. Its use had the advantage that possible charge transfer states would also be adequately treated. For a qualitative assignment of the experimental bands all methods seem to be appropriate.

Description of the Photolytic and Thermal N,O Bond Cleavage. Visible light absorption of *N*-(methoxy)pyridine-2(1*H*)-thione **1b** furnishes the methoxyl and the pyridyl-2-sulfanyl radical (**3**). In a similar way, $CH_3O^{\bullet}$ and the thiazyl-2-sulfanyl radical (**4**) are formed upon near-UV excitation of *N*-(methoxy)thiazole-2(3*H*)-thione **2b** (Figure 2).

The potential energy curves (see theoretical details) associated with the N,O homolysis of *N*-(methoxy)thiazole-2(3*H*)-thione (**2b**) starting from different states are depicted in Figure 3. All curves of the excited states, $T_1//T_1$, $S_1//T_1$, and $S_2//T_1$ are repulsive with respect to the N,O bond thus leading to a direct homolysis of this connectivity. The T_1 state correlates with the energetically lowest dissociation channel while S_1 and S_2 are connected with the next two higher pathways (Figure 3). It should be noted that the energetically lowest and the next higher dissociation channel are nearly degenerated ($\Delta E = 37$ cm^{-1}, see below). For a thermally induced cleavage along the S_0 state, the computed dissociation energy is 1.65 eV (159 kJ mol^{-1}).[53]

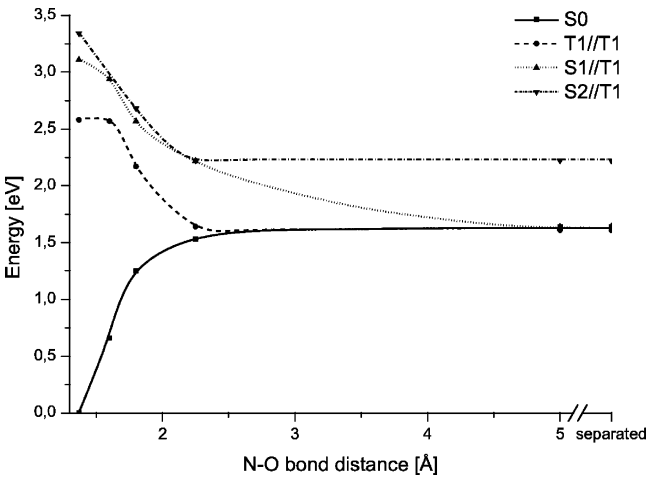

Figure 3. Potential curves for the thermal and photolytic N,O homolysis in *N*-(methoxy)thiazole-2(3*H*)-thione (**2b**) (CASPT2/cc-pVTZ, see also text).

Near-UV absorption of *N*-(methoxy)thiazole-2(3*H*)-thione **2b** will populate primarily the S_2 and probably not the S_1 state due to the significant difference in oscillator strengths of transitions going into these states starting from S_0 at the equilibrium geometry (Table 3). A N,O homolysis in **2b** along the S_2 state formally provides the thiazyl-2-sulfanyl radical (**4**) in its first excited state, while the methoxyl radical is formed in its electronic ground state. The energetic positioning of this third channel is computed as the vertical excitation energy of the thiazyl-2-sulfanyl radical (**4**). The corresponding orbitals (see Supporting Information) indicate that the unpaired electron is predominantly located at the exocyclic sulfur atom in **4**. However, the photochemically induced homolysis of the N,O bond in thione **2b** along the S_2 state is unlikely to occur. The very small energy gap between $S_1//T_1$ and $S_2//T_1$ at $R_{N,O} = 2.25$ Å and the shape of both curves clearly indicate a crossing of both states.[54] Due to this a fast relaxation $S_2 \rightarrow S_1$ can be expected. Even if no conical intersection exists the tiny energy gap would lead to an efficient quenching from the S_2 to the S_1 state.

Once relaxation of the molecule into the S_1 state has occurred, it can cross into the energetically lower state T_1 because the two states are coupled via spin−orbit interaction. On the other hand, dissociation starting from the S_1 level is also feasible because this state is repulsive with respect to the N,O connectivity. Starting from the S_1 level, the methoxyl radical is generated in its first excited state and the thiazyl-2-sulfanyl

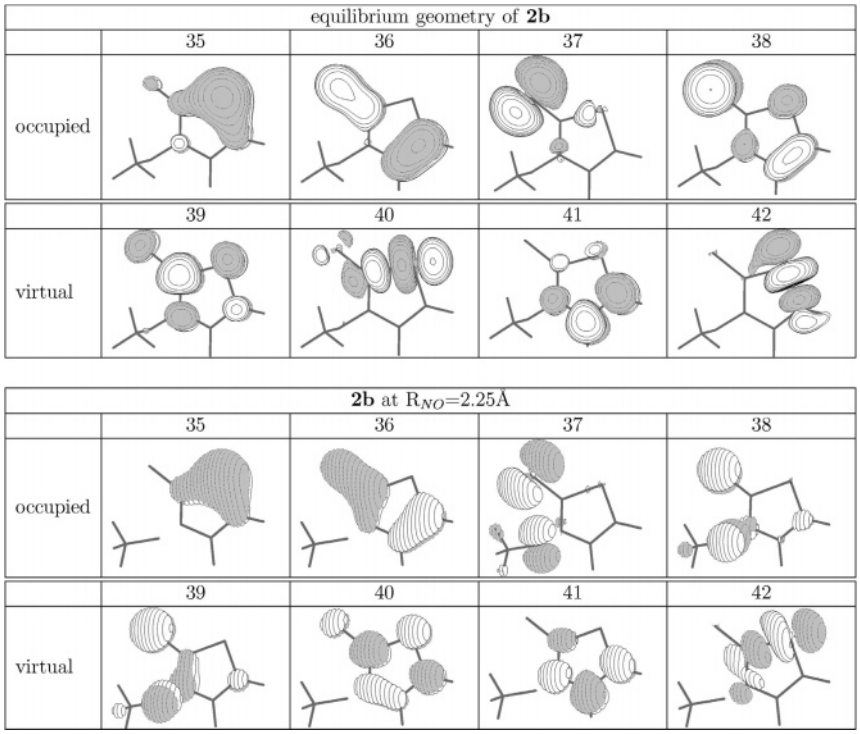

Figure 4. Relevant orbitals to describe the photolytic or thermal N,O homolysis in *N*-(methoxy)thiazole-2(3*H*)-thione (**2b**) (see also text).

radical (**4**) in its electronic ground state. A cleavage along the T_1 state would generate both fragments in their electronic ground states.

For the reactivity of the generated radicals it is irrelevant whether the cleavage proceeds along the S_1 or along the T_1 state since both lower channels are connected with the ground state X^2E of the methoxyl radical. Due to the Jahn−Teller distortion the X^2E state splits into a $^2A'$ (connected with the homolysis along the T_1 state) and a $^2A''$ (connected with the S_1 state) component. According to extended MR-CI calculations of Höper et al.,[52] the equilibrium geometry of the $^2A'$ component lies only about 200 cm^{-1} (0.02 eV) below the C_{3v} geometry and only 37 cm^{-1} below the equilibrium geometry of the $^2A''$. Due to this near degeneracy and since both channels are strongly coupled via rovibronic effects, in both cases a very fast relaxation to the lowest channel (both fragments in their ground state) will take place. As a consequence the arising methoxyl radical is generated in its electronic ground state no matter whether the cleavage proceeds along the S_1 or along the T_1 state. The same arguments are valid for other alkoxyl radicals that are formed in photochemically induced reactions from *N*-(alkoxy)thiazole-2(3*H*)-thiones. For these molecules the degeneracy of the X^2E state is lifted thus leading to small energy gaps between the ground state X and the first excited state $\tilde{A}$.[55] For the ethoxyl radical, for example, the experimental adiabatic $\tilde{A}-X$ excitation energy is 355 cm^{-1} (0.04 eV).[56] For the T conformer of 1-propoxyl radical a value of 320 cm^{-1} (0.04 eV) was measured.[56] Nevertheless the strong coupling between both low-lying states remains.

Variations in the orbitals along the N,O reaction coordinate are shown in Figure 4. For the equilibrium geometry it is seen that the orbitals are primarily located at the heterocyclic core and the thiocarbonyl group. None of the low-lying virtual or high-lying occupied orbitals possess density at the O atom. Therefore, none of these orbitals reflect an antibonding character with respect to the N,O bond. Such orbitals do not develop until the course of the N,O stretch ($R_{N,O}$ = 2.25 Å, Figure 4).

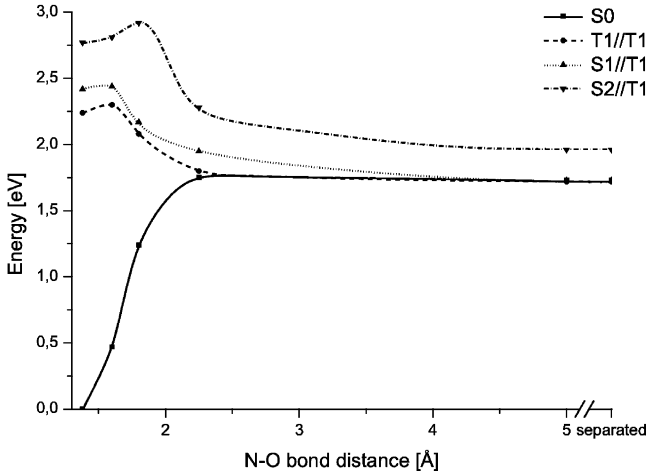

Figure 5. Potential curves for the thermal and photolytic N,O homolysis in *N*-(methoxy)pyridine-2(1*H*)-thione (**1b**) (CASPT2/cc-pVTZ, see also text).

The computed potential energy curves characterizing the thermally and the photochemically induced N,O homolysis in *N*-(methoxy)pyridine-2(1*H*)-thione (**1b**) are displayed in Figure 5. The properties of the S_2 state are of major interest for the chemistry that follows. It is the only state that is populated via near-UV excitation in a transition starting from the ground state that exhibits significant oscillator strength. Relevant orbitals for the equilibrium geometry and for $R_{N,O}$ = 2.25 Å can be taken from the Supporting Information. For the thermal cleavage along the S_0 ground state, the computed dissociation energy is 1.71 eV (168 kJ mol^{-1}).[53] The main difference between the pyridinethione **1b** and thiazolethione **2b** is the shape of the $S_2//T_1$ curve. For the thiazole derivative **2b**, this curve shows a repulsive shape. For pyridinethione **1b**, the fragmentation from S_2 is hindered by a small barrier of about 0.12 eV (12 kJ mol^{-1}). Furthermore, the energy difference between the $S_2//T_1$ and $S_1//T_1$ curves (0.4−0.6 eV) is larger than for thiazolethione **2b** (<0.1 eV) and does not at all indicate a conical intersection between

both states. The larger energy gap between the $S_2//T_1$ and $S_1//T_1$ curves could to some extent slow the relaxation from the S_2 to the S_1 state in pyridinethione **1b**. Since a direct fragmentation via the higher energy dissociation channel experiences a small energy barrier, we expect that a relaxation into the S_1 state will also occur for this compound as for example predicted by Kasha's rule.[57]

Similar to the situation in thiazolethione **2b**, the $S_1//T_1$ and $T_1//T_1$ curves in pyridinethione **1b** are within a first approximation parallel. The energy gap for the two curves is, however, considerably smaller (ca. 0.2 eV) than for the thiazole derivative **2b** (0.6−1.0 eV). As a consequence, it is expected that relaxation from the S_1 state into the T_1 state is more efficient in pyridinethione **1b**. Since a strong rovibronic coupling between both lowest lying dissociation channels occurs, the radicals that are formed from the dissociation reaction end up in their electronic ground state, regardless whether they originate from a N,O homolysis in the S_1 or the T_1 state.

The reason for the different chemistry that follows upon near-UV/vis excitation of, e.g., substituted *N*-(4-penten-1-oxy)-pyridine-2(1*H*)-thione and the corresponding *N*-(4-penten-1-oxyl)-4-methylthiazole-2(3*H*)-thione in the absence of efficient trapping reagents may be explained on the basis of differences in the excess energy of the radicals formed from both types of *O*-radical precursors. For *N*-(methoxy)thiazole-2(3*H*)-thione **2b**, the S_2 state, which according to the present results is predicted to be the starting point for the major route of N,O homolysis, is located 3.86 eV above the S_0 state. For *N*-(methoxy)pyridine-2(1*H*)-thione **1b**, an $S_0 \rightarrow S_2$ excitation energy of 3.27 eV has been computed. Taking the computed N,O dissociation energies of 1.65 eV (for **2b**) and 1.71 eV (for **1b**) into account, we predict that the radical fragments show an excess energy of 2.21 eV, if generated from thiazolethione **2b**, and 1.56 eV, if obtained from pyridinethione **1b**. For thiazolethione **2b**, we find a very efficient quenching process from the S_2 to the S_1 state due to a possible conical intersection at $R_{N,O} = 2.25$ Å. For pyridinethione **1b**, the $S_2 \rightarrow S_1$ transition occurs probably slower since the two potential curves are well separated along the whole N,O reaction coordinate. Assuming that energy dissipation occurs in the time it takes for the S_2-excited thione **1b** to relax into the S_1 state, the combined excess energy of radical **3** and the methoxyl radical would be even lower than 1.5 eV. In any case it is considerably lower than the excess energy predicted for radicals originating from **2b** (2.21 eV). This difference in excess energies could be one of the reasons why mediators are much more important for an efficient application of derivatives of *N*-(methoxy)thiazole-2(3*H*)-thione **2b** in *O*-radical-transformations than for the application of *N*-(alkoxy)pyridine-2(1*H*)-thiones **1b** in efficient chain reactions.

Comparison of the Applied Theoretical Approaches for a Computational Analysis of Thermally and Photochemically Induced N,O Homolysis of Pyridinethione 1b and Thiazolethione 2b. The CASPT2 approach provides very accurate results, but it is too expensive to be applicable to studying the N,O homolysis for systems with large substituents. TD-DFT is less expensive, but the question arises whether they are sufficiently accurate. The results obtained with the B3LYP functional are given in Figure 6 (for results using other functionals and for the performance of the applied theoretical methods for the computational analysis of pyridinethione **1b**, see the Supporting Information). Like the CASPT2 approach, the B3LYP functional predicts repulsive $T_1//T_1$, $S_1//T_1$, and $S_2//T_1$ curves (Figure 6). With increasing N,O distances, however, the energy gaps between the various states become much larger

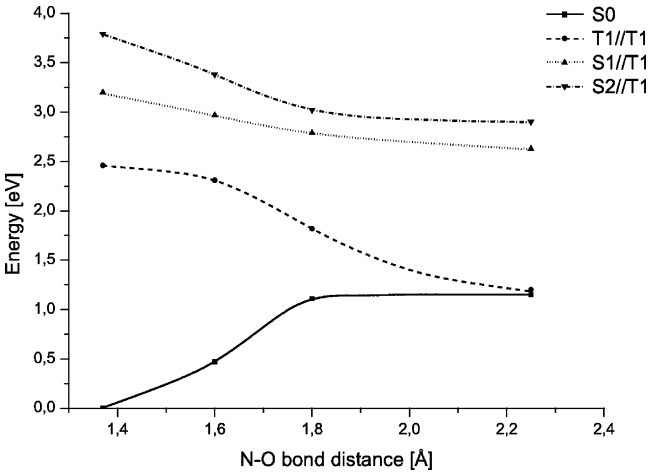

Figure 6. Potential curves for the thermal and photolytic N,O homolysis in *N*-(methoxy)thiazole-2(3*H*)-thione (**2b**) (B3LYP/TZVP).

than those predicted by CASPT2. Obviously B3LYP is not adequate to describe the complicated electronic structure of the $S_1//T_1$ or $S_2//T_1$ states for stretched N,O bonds. Although these states are far too high in energy, the positioning of the $T_1//T_1$ state for **2b** is in very good agreement with the CASPT2 results.

The RI-CC2 approach was found to give quite reliable vertical excitation energies for the singlet states. Since it represents a single reference method, problems are expected for the description of the photolytic dissociation. This is indeed the case. The computed curves of the S_1 and S_2 states resemble those obtained with the DFT approaches (see Supporting Information).

Summary

In the present paper we have studied the mechanism of thermally and photochemically induced N,O homolysis in *N*-(methoxy)pyridine-2(1*H*)-thione (**1b**) and *N*-(methoxy)thiazole-2(3*H*)-thione (**2b**). Both compounds constitute parent structures of important groups of alkoxyl radical precursors. CASSCF, CASPT2, TD-DFT, and RI-CC2 were tested with respect to their ability to describe the dissociation process and the vertical excitations. Computations were performed for the first three electronic states of *N*-(methoxy)pyridine-2(1*H*)-thione (**1b**) and *N*-(methoxy)thiazole-2(3*H*)-thione (**2b**) as well as for the *N*-(hydroxy) derivatives **1a** and **2a**. The complete active space approach in association with the MS-CASPT2 ansatz gives accurate descriptions of experimental electronic excitation spectra. The same is found for RI-CC2 which in comparison to CASPT2 predicts slightly higher vertical excitation energies (0.1 to 0.3 eV). The time-dependent DFT results are very dependent on the choice of the functional and the examined state. The BLYP functional in general underestimates the excitation energies systematically while the BHLYP overestimates them. The Becke three-parameter functional (B3LYP) and PBE0 in most cases give excitation energies in the same region as CASPT2.

For the thermal and the photolytic bond dissociation process, only the CASPT2 method provides reasonable results. The near-UV-induced N,O homolysis of thiones **1b** and **2b** will start from the S_2 states. In both compounds it is the only state that exhibits significant oscillator strengths, i.e., will be populated upon light absorption. N,O homolysis in the S_2 state occurs with no energy barrier (for **2b**) or with a very small barrier (for **1b**). This step furnishes excited sulfanyl radicals **3** (from **1b**) or **4** (from **2b**) and the methoxyl radical in its electronic ground state. The computed S_2 and the S_1 curves point to a conical intersection

between the S_1 and S_2 states which will enable an efficient $S_2 \rightarrow S_1$ relaxation for **2b**. For both thiones **1b** and **2b**, the S_1 state is repulsive with respect to the N,O bond. Relaxation of S_1-excited thiones **1b** and **2b** into the T_1 state is feasible via spin−orbit interaction. The T_1 state leads to the lowest fragmentation channel. For the noninteracting fragments, the S_1 and T_1 channels correspond to the ^{2}E ground state of the methoxyl radical. As a consequence the explicit pathway (via S_1 or T_1) is irrelevant for the subsequent chemistry since the relaxation to the ground state of the alkoxylradical will be faster than its chemical reactions.

The data from the present study outline that *O*-radicals generated from structurally closely related precursors, i.e., the *N*-(alkoxy)pyridine-2(1*H*)-thiones on one side and the *N*-(alkoxy)-thiazole-2(3*H*)thiones on the other side, may exhibit different excess energies. It is tempting to correlate these energetic differences with the different chemical behaviors of the groups of heterocyclic thiones if photolyzed in the absence of additional trapping reagents.

Supporting Information Available: The Supporting Information contains the cartesian coordinates of the ground states obtained with RI-BLYP/SVP and RI-MP2/cc-pVTZ, followed by the absolute energies obtained with various methods (B3LYP, BLYP, BHLYP, PBEO, and RICC2) and various basis sets (TZVP, TZVP+diffuse, cc-pVTZ, and cc-pVTZ+diffuse). This information is given in the order **1a**, **1b**, **2a**, and **2b**. Then, the data for the homolysis are summarized. This includes the geometries optimized along the reaction path on the ground state. For each geometry the computed total energies for the four lowest lying electronic states are given. The same information for the reaction path on the lowest triplet and on the first excited singlet state follows. In addition figures describing the homolysis computed with the CC2 method and the most important orbitals are given. Finally information about the used basis sets and the influence of the basis set variations on the excitation energies is summarized. This material is available free of charge via the Internet at http://pubs.acs.org.

References and Notes

(1) Adam, W.; Hartung, J.; Okamoto, H.; Saha-Möller, C. R.; Špehar, K. *Photochem. Photobiol.* **2000**, *72*, 619−624.

(2) Adam, W.; Hartung, J.; Okamoto, H.; Marquardt, S.; Nau, W. M.; Pischel, U.; Saha-Möller, C. R.; Špehar, K. *J. Org. Chem.* **2002**, *67*, 6041−6049.

(3) Aveline, B. M.; Redmond, R. W. *Photochem. Photobiol.* **1998**, *68*, 266−275.

(4) Hartung, J.; Gallou, F. J. *Org. Chem.* **1995**, *60*, 6706−6716.

(5) Boivin, J.; Crépon, E.; Zard, S. Z. *Tetrahedron Lett.* **1990**, *31*, 6869−6872.

(6) Hartung, J.; Kneuer, R. *Eur. J. Org. Chem.* **2000**, 1677−1683.

(7) Renaud, P.; Gerster, M. *Angew. Chem.* **1998**, *110*, 2704−2722.

(8) Porter, N. A.; Giese, B.; Curran, D. P. *Acc. Chem. Res.* **1991**, *24*, 296−304.

(9) Esker, J. L.; Newcomb, M. *Adv. Heterocycl. Chem.* **1993**, *58*, 1−45.

(10) (a) Barton, D. H. R.; Parekh, S. I. *Half a Century of Free Radical Chemistry*; Cambridge, University Press: Cambridge, 1993. (b) Motherwell, W. B.; Imboden, C. In *Radicals in Organic Synthesis;* Renaud, P., Sibi, M. P., Eds.; Wiley-VCH: Weinheim, 2000; Vol. 1, pp 109−134. (c) Crich, D.; Quintero, L. *Chem. Rev.* **1989**, *89*, 1413−1432. (d) Hartung, J. *Eur. J. Org. Chem.* **2001**, 619−632.

(11) Hartung, J.; Gottwald, T.; Špehar, K. *Synthesis* **2002**, 1469−1498.

(12) Hartung, J.; Špehar, K.; Svoboda, I.; Fuess, H.; Arnone, M.; Engels, B. *Eur. J. Org. Chem.* **2005**, 869−881.

(13) Bauernschmitt, R.; Ahlrichs, R. *J. Am. Chem. Soc.* **1998**, *120*, 5052−5059.

(14) Bauernschmitt, R.; Ahlrichs, R. *Chem. Phys. Lett.* **1996**, *256*, 454−464.

(15) Becke, A. D. *Phys. Rev. A* **1988**, *38*, 3098−3100.

(16) Lee, C.; Yang, W.; Parr, R. G. *Phys. Rev. B* **1988**, *37*, 785−789.

(17) Becke, A. D. *J. Chem. Phys.* **1993**, *98*, 5648−5652.

(18) Hupp, T.; Görling, A.; Engels, B. *J. Chem. Phys.* **2003**, *119*, 11591−11601.

(19) Grimme, S. Calculations of the Electronic Spectra of Large Molecules; In *Reviews in Computational Chemistry Vol. 20*; Lipkowitz, K. B., Ed.; John Whyley & Sons Ltd.: Chester, U.K., 2004; pp 153−218.

(20) Roos, B. O.; Taylor, P. R.; Siegbahn, P. E. M. *Chem. Phys.* **1980**, *48*, 157−173.

(21) Roos, B. O. The complete active space self-consistent field method and its applications in electronic structure calculations. In *Advances in Chemical Physics; Ab Initio methodes in Quantum Chemistry − II*; Laweley, K. B., Ed.; John Whyley & Sons Ltd., Chester, U.K., 1987; p 139.

(22) Andersson, K.; Malmqvist, P.-Å.; Roos, B. O. *J. Chem. Phys.* **1992**, *96*, 1218−1226.

(23) Andersson, K.; Malmqvist, P.-Å.; Roos, B. O.; Sadley, A. J.; Wolinski, K. *J. Phys. Chem.* **1990**, *94*, 5483−5488.

(24) Grimme, S.; Parac, M. *ChemPhysChem.* **2003**, *3*, 292−295.

(25) Dreuw, A.; Weisman, J. A.; Head-Gordon, M. *J. Chem. Phys.* **2003**, *119*, 2943−2946.

(26) Dreuw, A.; Head-Gordon, M. *J. Am. Chem. Soc.* **2004**, *126*, 4007−4016.

(27) Petiau, M.; Fabian, J. *THEOCHEM* **2001**, *538*, 253−260.

(28) Christiansen, O.; Koch, H.; Jørgensen, P. *Chem. Phys. Lett.* **1995**, *243*, 409−418.

(29) Christiansen, O.; Koch, H.; Jørgensen, P.; Olsen, J. *Chem. Phys. Lett.* **1995**, *244*, 75−82.

(30) Christiansen, O.; Koch, H.; Jørgensen, P.; Helgaker, T. *Chem. Phys. Lett.* **1996**, *263*, 530−539.

(31) Fliegl, H.; Köhn, A.; Hättig, C.; Ahlrichs, R. *J. Am. Chem. Soc.* **2004**, *125*, 9821−9827.

(32) Eichkorn, K.; Treutler, O.; Öhm, H.; Häser, M.; Ahlrichs, R. *Chem. Phys. Lett.* **1995**, *242*, 652−660.

(33) Vahtras, O.; Almlöf, J.; Feyereisen, M. W. *Chem. Phys. Lett.* **1993**, *213*, 514−518.

(34) Hättig, C.; Weigend, F. *J. Chem. Phys.* **2000**, *113*, 5154−5161.

(35) Hättig, C.; Köhn, A. *J. Chem. Phys.* **2002**, *117*, 6939−6951.

(36) Ahlrichs, R.; Bär, M.; Baron, H.-P.; Bauernschmitt, R.; Böcker, S.; Ehrig, M.; Eichkorn, K.; Elliott, S.; Haase, F.; Häser, M.; Horn, H.; Huber, C.; Huniar, U.; Kattannek, M.; Kölmel, C.; Kollwitz, M.; Ochsenfeld, C.; Öhm, H.; Schäfer, A.; Schneider, U.; Treutler, O.; von Arnim, M.; Weigend, F.; Weis, P.; Weiss, H. *TURBOMOLE*; Quantum Chemistry Group, University of Karlsruhe: Germany, 1988.

(37) Andersson, K.; Barysz, M.; Bernhardsson, A.; Blomberg, M. R. A.; Cooper, D. L.; Fleig, T.; Fülcher, C. M. P.; de Graaf, C.; Hess, B. A.; Karlström, G.; Lindh, R.; Malmqvist, P.-Å.; Neogrády, P.; Olsen, J.; Roos, B. O.; Sadley, A. J.; Schütz, M.; Schimmelpfennig, B.; Seijo, L.; Serrano-Andrés, L.; Siegbahn, P. E. M.; Stålring, J.; Thorsteinsson, T.; Veryazov, V.; Widmark, P.-O. *MOLCAS*, version 5; Lund University: Sweden, 2000.

(38) Schäfer, A.; Horn, H.; Ahlrichs, R. *J. Chem. Phys.* **1992**, *97*, 2571−2577.

(39) Weigend, F.; Köhn, A.; Hättig, C. *J. Chem. Phys.* **2002**, *116*, 3175−3183.

(40) Andersson, K. *Theor. Chim. Acta* **1995**, *91*, 31−46.

(41) Finley, J.; Malmqvist, P.-Å.; Roos, B. O.; Serrano-Andrés, L. *Chem. Phys. Lett.* **1998**, *288*, 299−306.

(42) Woon, D. A.; Dunning, T. H., Jr. *J. Chem. Phys.* **1993**, *98*, 1358−1371.

(43) Dunning, T. H., Jr. *J. Chem. Phys.* **1989**, *90*, 1007−1023.

(44) Malmqvist, P.-Å.; Roos, B. O. *Chem. Phys. Lett.* **1989**, *155*, 189−194.

(45) Schäfer, A.; Huber, C.; Ahlrichs, R. *J. Chem. Phys.* **1992**, *100*, 5829−5835.

(46) Becke, A. D. *J. Chem. Phys.* **1992**, *98*, 1372−1377.

(47) Perdew, J. P.; Ernzerhof, M.; Burke, K. *J. Chem. Phys.* **1996**, *105*, 9982−9985.

(48) Perdew, J. P.; Burke, K.; Ernzerhof, M. *Phys. Rev. Lett.* **1996**, *77*, 3865−3868.

(49) Bauernschmitt, R.; Häsler, M.; Treutler, O.; Ahlrichs, R. *Chem. Phys. Lett.* **1997**, *264*, 573−578.

(50) Rappoport, D.; Furche, F. *J. Chem. Phys.* **2005**, *122*, 064105.

(51) Furche, F.; Ahlrichs, R. *J. Chem. Phys.* **2002**, *117*, 7433−7447.

(52) Höper, U.; Botschwina, P.; Köppel, H. *J. Chem. Phys.* **2000**, *112*, 4132−4142.

(53) For the computations employing the CASPT2 approach, the dissociation energies were computed as the difference between the equilibrium geometries and $R_{NO} = 5$ Å.

(54) An analysis of wave functions and orbitals also indicate such a crossing; however, a final proof was not possible.

(55) Tarczay, G.; Gopalakrishnan, S.; Miller, T. A. *J. Mol. Spectrosc.* **2003**, *220* 276−290.

(56) Ramond, T. M.; Davico, G. E.; Schwartz, R. L.; Lineberger, W. C. *J. Chem. Phys.* **2000**, *112*, 1158−1169.

(57) Kasha, M. *Discuss. Faraday Soc.* **1950**, *9*, 14−19.